SF2A 2006
D. Barret, F. Casoli, T. Contini, G. Lagache, A. Lecavelier, and L. Pagani (eds)

SHOCK WAVES AND ELECTRON DYNAMICS

Philippe Savoini[1] and Bertrand Lembege[1]

Abstract. Collisionless shock waves are observed in different regions of our universe. They are a good candidat for the formation of high energy particles through different processes like the well-known first/second Fermi processes. Such acceleration mechanisms are not alone and others can be observed when one takes into account the internal shock structure. As an example, we will focus on the impact of different processes on electron acceleration such as (a) shock front inhomogeneity, (b) shock front instationarity and (c) curvature effects of the shock front in the case of a supercritical quasi-perpendicular.

Numerical simulations allow us to observed precisely the time/space shock and the related evolution the particle dynamic. A two-dimensional electromagnetic full particle code is used in order to analyze electron self-consistently. It is shown that, for planar shock waves, bursts of energetic backstreaming electrons are formed in time by the shock reformation; in addition, these bursts are not uniform in space but are modulated by the shock rippling when electrons are reflected by the shock front. In addition, when the curvature effects are included, we observe the formation of backstreaming electrons which leads to the formation of "bump-in -tail" in the parallel distribution as we can divided in two different components: (i) a low parallel kinetic energy component (high percentage of electrons density) corresponding to mirrored electrons characterized by a loss-cone signature and (ii) a high parallel energy component (low percentage of electrons density) corresponding to backstreaming electrons characterized by a field aligned beam signature.

1 Introduction

Formation of energetic electrons by a collisionless shock is of very wide interest in magnetospheric shocks, as well as for interplanetary shocks and shocks in solar physics related to coronal mass ejection (CME) events. These hit the shock either when carried with the flowing solar wind (as for terrestrial bow shock) or when the piston-like shock is expanding within the interplanetary medium (as for shocks related to CME). While interacting with the shock front, electrons divide into two classes: electrons are either transmitted through or are reflected against the shock front. Energetic reflected electrons play an important role since they strongly interact with the upstream ambiant plasma and may be responsible for electrostatic and electromagnetic wave emissions.

On the other hand, the study of the electron acceleration processes are complicated by the intrinsic characteristics of a collisionless shock wave. In particular, *(i)* the **nonstationary** of the shock front or in the other word, the time variation of the shock front features and *(ii)* the geometry properties of the bow shock which has a two dimensional **curved pattern** and which can modify the effectiveness of the acceleration process.

In order to address these different characteristics, the present paper focuses on results obtained with the help of a full-particle code where electrons and ions dynamics (and associated scalelengths) are fully included in a self-consistent way.

2 Salient Features of a shock wave

The solar wind encounters the magnetic field obstacle of the terrestrial magnetosphere whereas it is in supersonic regime. Then, a bow shock is formed ahead of the magnetopause (limit of the terrestrial magnetic field). Such a frontier acts as an energy converter, transforming the bulk flow of the solar wind into local plasma acceleration and heating.

[1] CETP/UVSQ, 10-12, Avenue de l'Europe, 78140 Vélizy

Over the past 3 decades, our knowledge of collisionless shocks in general and planetary bow shocks in particular has greatly increased (see, e.g., review articles by Tsurutani and Stone, 1985; Russell, 1995 and lembege et al., 2004). Briefly, we classify a bow shock with two parameters :

(i) The propagation angle (θ_{Bn}) defined between the angle between the interplanetary magnetic field and the shock normal. Two distinct domains of propagation can be defined : a quasi-perpendicular $90° \leq \theta_{Bn} \leq 45°$ and a quasi-parallel $45° \leq \theta_{Bn} \leq 0°$ domain. Within each range, the shape of the shock front, its scale and dynamics are totally different. So do, the dissipation processes in the two regimes, although in both cases ion heating is the dominant source of dissipation.

(i) The Mach number (hereafter, $M_A = V_{sw}/V_A$ where V_{sw} is the Solar Wind bulk velocity). This parameter stands for the strength of the shock (i.e. the energy available) which can be converted into thermal energy and/or particle acceleration. We can define two different propagation regimes. The subcritical regime ($M_A \leq M_A^\star$, $M_A^\star$ is the so-called first critical Mach number) where the dissipation is mainly due to the electron population ("anomalous" resistivity) and is driven by the electric current supporting the strong fields gradients at the ramp. The supercritical regime ($M_A \geq M_A^\star$) where an additional source of dissipation is necessary and is associated to the ion population ("anomalous" viscosity). In the last regime, a substantial fraction of the incoming upstream ions are reflected at the shock front.

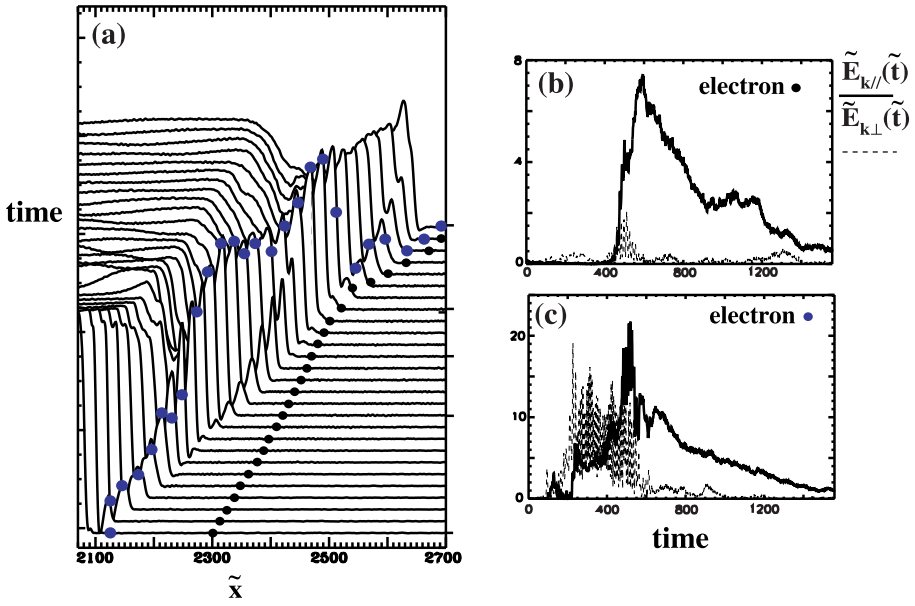

Fig. 1. (a) Stackplots of the y-averaged magnetic field B_{tz} at different times of the run from $t = 0$ to $15\omega_{ci}^{-1}$ of a planar supercritical shock wave with $\theta_{Bn} = 55°$. As an example, the x location of two reflected electrons have been reported to evidence the magnetic mirror acceleration (panel b) and the resonant acceleration (panel c) where have been plotted the parallel (solid line) and perpendicular (dashed line) kinetic energy of the particles (from Lembege and Savoini, 2002).

In the present paper, we will focus only on a small part of the overall shock front-particles interactions. In particular, some results will be presented onto the electron reflection processes observed at a supercritical ($M_A \geq M_A^\star$), quasi-perpendicular ($90° \leq \theta_{Bn} \leq 45°$) collisionless shock wave as plotted in Figure 1.

2.1 Non stationarity of the shock wave

Unlike fluid, local description of the kinetic dissipation via the reflected ions can be much more dynamic. Full particle simulations (Lembege and Savoini, 1992) evidenced a nonstationarity of the shock front along the shock normal, i.e. a self-reformation of the front which has been invoked to explain some experimental datas (Horbury et al., 2001).

Such a behavior can be explained in terms of reflected ions accumulation in front of the ramp. They form a foot in the magnetic field (in front of the ramp) and as time goes on, more and more reflected ions accumulate, leading to the formation of a new shock front, at a location about a foot length in front of the original shock

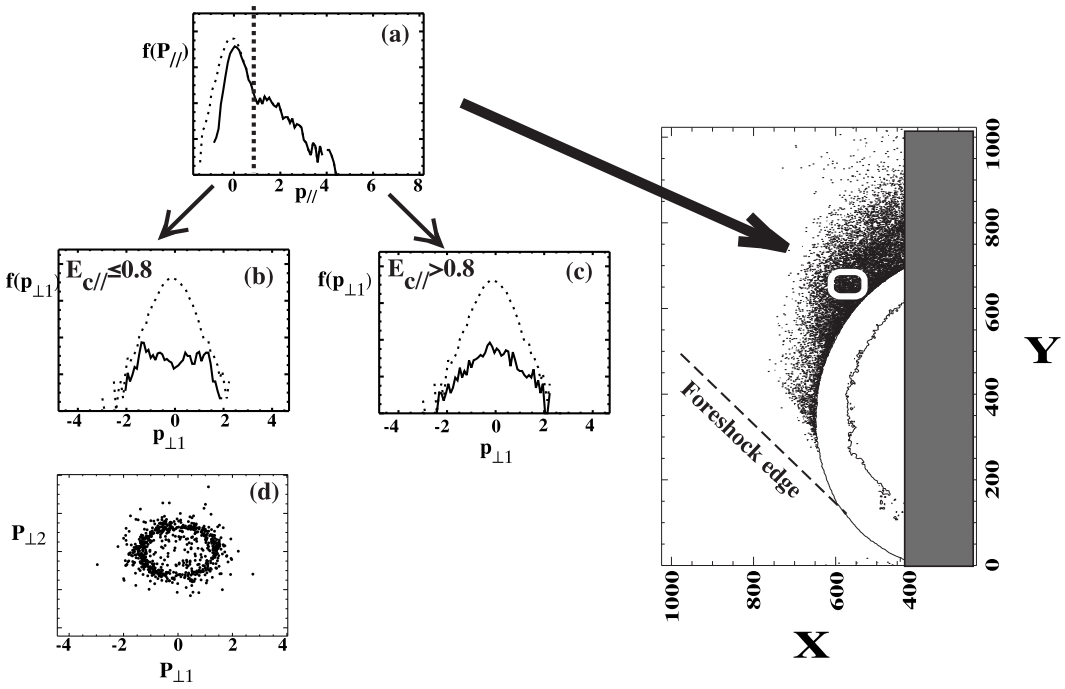

Fig. 2. Location of foreshock electrons within the simulation plane at time $1.1\tau_{ci}$. A local electron distribution function (in log scale) has been measured within the foreshock region (white square). Total (dotted line) and backstreaming (solid line) parallel electron distributions $f(p_{//})$ are represented in panel a. Panels b and c show the corresponding perpendicular distribution function splitted according to the parallel energy criteria (vertical dotted line): the low energy population (panel b) and the high energy population (panel c), respectively. The last panel (panel d) plots the perpendicular velocity space of the low energy population (from Savoini and Lembege, 2001).

front. This entire process is repeated through an ion gyroperiod, periodically as illustrated by figure 1a which shows the stackplot of the main magnetic component $\widetilde{B}_{tz}$ for different times.

In addition, at small scales, the nonstationarity of the shock turns into shock-front rippling along the shock front. For $\theta_{Bn} = 90°$, this rippling is associated to instabilities triggered by cross-field currents supporting the large fields gradient at the front and belong to the lower hybrid family (Lembege and Savoini, 1992). This rippling persists for oblique propagation $\theta_{Bn} < 90°$ although a clear identification of its origin is not complete.

2.2 Curved shock pattern

In addition, the curved pattern of the bow shock is associated to a particular region, the foreshock. This is the region of space extending between the curved shock layer and the upstream magnetic field lines tangent to the shock. It is characterized by the presence of energetic particles backstreaming away from the shock front along interplanetary magnetic field lines. This region has been extensively studied both theoretically (Leroy and Mangeney, 1984; Wu, 1984, Fitzenreiter et al., 1990) and experimentally (Feldman et al., 1983; Klimas, 1985; Fitzenreiter et al., 1996, Yin et al., 1998) but only recent $2-D$ numerical simulations succeeded to analyse the electron foreshock by a self-consistent approach(Savoini and Lembege, 2001). One example is reported in figure 2a for a portion of the quasi-perpendicular bow shock ($90° \leq \theta_{Bn} \leq 65°$) showing the backstreaming electrons in the upstream region.

3 Impact of the shock front properties on the Electron reflection processes

Both nonstationarity and curved pattern of the shock front has to be take into account to understand in details the electron acceleration/reflection processes. Both time and spatial shock front nonstationarities appear to have a strong impact on the electron reflection process. Lembege and Savoini (2002) evidence cyclic energetic

reflected electron burst (one in each cyclic reformation of the shock front) which are not distributed uniformly in space. Indeed, packs of electrons are well formed along the rippled shock front and escape away from the shock in time. Numerical simulations allow us to go further in the analysis and show roughly two distinct mechanisms of acceleration into the electron reflection process:

(i) The **Fermi acceleration** (magnetic mirror reflection). Such a reflection is illustrated on figure 1b, for a planar shock, by an electron (black point) which receives mainly a kick from the shock. As a result, its kinetic energy gain takes a noticeable value ($\approx 8E_{ik}$ where E_{ik} is its initial kinetic energy) along the local magnetic field. No noticeable perpendicular gain is observed and consequently its magnetic momentum is almost conserved which is a characteristic of the magnetic-mirror-type reflection.

(ii) The **resonant acceleration**. A good example of such a mechanism has been plotted in figure 1c. In this case, the electron goes deeper into the shock front where it is trapped within the electrostatic field built at the ramp. The energy transfer becomes quite strong both in parallel and perpendicular directions. At later times the electron can leave the shock front when it has gained enough energy.

It is interesting to point out that some electrons are overcome at later time by the front when their escaping velocity are lower than the shock front velocity. In this case, we observe multibounce until electrons gain enough energy to escape into the upstream region.

Finally, it is interesting to analyse energetic reflected electrons when the curved pattern of the shock is fully involved. The two dimensional full-particle simulations allow us to recover all main features of the electron foreshock properties observed experimentaly (Fitzenreiter et al., 1990). Figure 2 shows *only* the electrons which have interacted with the bow shock and are backstreaming into the upstream region. The electron distribution functions computed locally in this region exhibits a characteristic bump-on-tail pattern (panel 2a) formed by these reflected electrons. Two different populations components can be clearly identified in terms of parallel kinetic energy gain. A low parallel energy population which evidences a characteristic perpendicular loss cone distribution function (panel 2b) due to the mirror reflection. Such a loss cone signature is clearly evidenced by a "ring-shape" formed in the local perpendicular velocity space (panel 2c). The high parallel energy population whose the local perpendicular distribution functions (panel 2c) do not exhibit any loss-cone feature, has to be formed by another acceleration mechanism such as the resonant acceleration previously described.

References

Balikhin, M. A., et al. 1997, Adv. Space. Res., 20, 729734

Feldman W. C. et al. 1983, J. Geophys. Res., 88, 96-110, 1983

Fitzenreiter, R. J. and J. D. Scudder and A. J. Klimas1 1990, J. Geophys. Res., 95, 4155417

Fitzenreiter, R. J. et al. 1996 Geophys. Res. Lett., 23, 12351238

Horbury, T. S. et al. 2001 Ann. Geophysicae, 19, 13991409

Klimas , A. J. 1985, in series Collisionless shocks in Heliosphere: Reviews of current research, Tsurutani, B., and R. Stone (Eds.), Geophys. Monogr. Ser., vol. 30, AGU, Washington, D. C

Krasnoselskikh, V. V., Lobzin V. V. , and Rozov V. B. 1990; in Proceeding of the Joint Varenna-Abastunami-ESA-Nagoya-Potsdam Workshop on Plasma Astrophysics Telavi, Georgia, USSR, ESA SP311, 103 107,

Lembege, B., and P. Savoini 1992, Phys. Fluids, 4, 35333548

Lembege, B. and Ph. Savoini 2002, J. Geophys. Res., 107, 1037

Lembege, B. et al. 2004 Space Sci. Rev., 110, 161226

Leroy M. M. and A. Mangeney 1984, Ann. Geophys., 2, 449456

Russell, C. T. (Ed.) 1995, Adv. in Space Res., Elsevier, New York

Savoini Ph. and B. Lembège 2001, J. Geophys. Res., 106, 1297512992

Tsurutani, B., and R. Stone (Eds.), Collisionless Shocks in the Heliosphere, Geophys. Monogr. Ser., vol. 30, AGU, Washington, D. C, 1985.

Wu, C. S. 1984, J. Geophys. Res., 89, 88578862

Yin, L. et al. 1998, J. Geophys. Res., 103, 2959529617